GAVIN PUBLISHERS

Archives of Petroleum & Environmental Biotechnology

Research Article

Żbik MS and Williams DJ. Arch Pet Environ Biotechnol 2017: 109
DOI: 10.29011/2574-7614.100109.

Influence of Physical Treatment on Kaolinite Floccule Microstructure

Marek Żbik* **and David Williams**

Geotechnical Engineering Centre, The University of Queensland, Australia

***Corresponding author:** Marek Żbik, Geotechnical Engineering Centre, The University of Queensland, Australia, Tel: +48 (22) 5531412; Email: marek.zbik@uw.edu.pl

Citation: Żbik MS and Williams DJ (2017) Influence of Physical Treatment on Kaolinite Floccule Microstructure. Arch Pet Environ Biotechnol 2017: 109. DOI: 10.29011/2574-7614.100109

Received Date: 26, April, 2017; **Accepted Date:** 4, May, 2017; **Published Date:** 6, May, 2017

Abstract

Microstructure investigation of kaolinite clay suspensions were conducted to understand better the poor settling and dewatering of clay rich mine tailings. The subject of testing was a 5 wt.% kaolinite (KGa-2) aqueous suspension treated by pH change, ultrasonic and microwave action, polymeric flocculent and steatite addition. Kaolinite suspensions were investigated using synchrotron powered Transmission X-ray Microscope with subsequent computer 3D reconstruction. Treatment results favour the microwave treatment over ultrasonic for better aggregate dispersion. Surprisingly, after the flocculent addition into the dispersed kaolinite slurry, particles were prevented from coagulation by polymer action. Best aggregation results were recorded at low pH, microwave treated and ultrasonic treated after small amounts of Smectite addition. Significant portion of the voids were found to be filled by air micro-bubbles which add buoyancy to the entire clay network, reinforcing it against gravitational sedimentation along with steric interaction inflicted by scaffolding-like clay platelets space network.

KeyWards: Clay suspension structure; Georgia Kaolinite; Kaolinite; Kaolinite flocculation; minerals processing

Introduction

The term “kaolin” is used to name soft rocks which consist of clay minerals from the kaolinite group, together with other minerals. The kaolinite group includes kaolinite, Nacrite, dickite and halloy site. All of these clays (except for halloy sites) have essentially the same composition and differ only in their crystal structure. Kaolinite belongs to secondary minerals which were produced by chemical transformation of primary igneous minerals such as feldspars and micas. Clay rich rocks, which have formed directly in place of primary minerals, are called primary deposits. Most Clays however undergo re deposition through water transport to different locations such as in lakes or lagoons where secondary deposits form. Kaolinite has a 1:1 structure with a single sheet of hydroxyls octahedral coordinated to aluminium cations linked through oxygen’s to a single layer of silica tetrahedral. The layered structure has a unit cell thickness of 0.713 nm [1].

The siloxane-like surface has pH-independent charge where as the octahedrally coordinated Al–OH sheet and the edge Al OH (and Si OH) sites have pH-dependent surface charges. The surface charge characteristics have been successfully modelled for this structure [2]. It is believed that the oxygen atoms at the basal surface of the siloxane-like sheets are hydrophobic whereas the edges and the surface of the octahedral sheets are hydrophilic [2,3].

Primary dewatering processes include aggregate formation, bridging flocculation, settling rate and bed height (density) before compression. This can be achieved by physico-chemical processes like aggregation, coagulation and flocculation which were clarified recently in Osipov and Sokolov (2013). Aggregation is usually understood as a process of formation larger and stable structural elements by primary particles connecting in Face to Face phase contacts and becoming unstable [4]. Coagulation is connected mostly with interaction between primary particles within dense suspensions (gels) resulting in Face to Edge (FE) and Edge to Edge (EE) coagulating type contacts. Flocculation also is seen as a process of building larger structural elements and some authors Van Olphen, 1977; Mitchell and Soga, 2005 relate this with coagulation. Others present flocculation as a separate type of coagulation to be achieved by flocculation using long chain polymers; however, this process is still not well understood. When solids concentra-

tion exceeds a certain value, the suspension gels and locks large and minute particles in a 3-D net work leaving clear supernatant layer above the compacting gel (usually above 2 wt.%). Inside the gelled suspension free settling is not observed but more or less restricted hindered compaction takes place. Denser suspensions (4 wt. %) are very slow to compact and many high clay fraction content soil samples gelled and resist settlement. Kotlyar (1970) [5] and O" Brayen (1998) [6] suggest but did not observe that particles in such gels are in constant contact with each other by creating a 3-D structure. Such a structure was reported in the first ever SEM observations of the clay particle in dilute suspensions Brayen (1998) [6] where kaolinite platelets were found to form networks with surrounding particles.The structure building phenomenon has been observed later in TXM Yin et al, (2006), [7].and Cryo-SEM investigation [8]. And the nano-size particles (Kotlyar et al 1996) [9] were believed to be responsible. It has been found that a concentration of only 1 to 1.5 vol. % of nano particles is required to produce a space filling, gel network. Presence of the extremely small particles (nano-colloids) in a suspension was reported to enhance sample flocculation (Kotlyar et al. 1998) [10]. Within fraction containing particles of diameters, less than 200 nm, suspended in 0.1 M NaCl solution, gelatin was instantaneous. It was observed that larger particles were frequently immobilized within voluminous network of gelled suspensions or floccs.

The gelled clay rich suspension has high water holding capacity. Water is encapsulated within inter-aggregate cellular microvoids. Such gelled suspension resists settling which was observed in many of our tests. Because of the lack of free sedimentation and well defined borders between flocc aggregates, specific information such as in situ aggregate density distribution and floccs dimensions are very difficult or impossible to determine. To help understand micro structural behavior of kaolinite gelled suspensions and to find a way of characterizing the effects of certain treatments, the microstructure investigation was conducted using a Transmission X-ray Microscope. Different microscopy techniques were developed during recent decades. The application of a high resolution transmission X-ray microscope (TXM), has increased with the availability of synchrotron photon sources. In the soft X-ray range (100eV – 1 ke V), a zone plate based TXM Yin et al, (2006) [11], has achieved a spatial resolution of 15 nm. This has been a big challenge in the hard X-ray region because of the difficulties in zone plate manufacturing. In this article, we are using the microscope constructed in the National Synchrotron Radiation Research Canter (NSRRC). Attwood (2006) [12] also described this method of nanotomography used in the present work. In this method, we combine two- dimensional images (2D) taken at different incident X-ray angles, allowing internal structures to be discerned with a spatial resolution of around 60 nanometers. Clay aggregates already studied by different X-ray microscopy methods as described by Niemeyer, (1994) [13]. This particular method using TXM with nanotomography was pioneered in the clay suspension nano-structure investigation by Żbik et al. (2008). [14].The big advantage of the TXM tomography is the possibility of observing clay microstructure in a water environment, limited artifacts and without sample pre-treatment. In the present work, synchrotron based TXM nanotomography method is shown in microstructure characterization of modified clay kaolinite suspensions.

Experimental Section

Kaolinite (KGa-2) chosen in the present study has been obtained from the Clay Minerals Society repository and is well characterised by Van Olphen and Fripiat, (1979) [4]. From the many parameters for this clay mineral, the action exchange capacity (CEC): 3.3 meq/100, and specific surface area: BET 23.50 +/- 0.06 m2/g were used as most applicable for this current study. This particular well studied kaolinite, originates from the lower tertiary period, County of Warren, State of Georgia, USA. This kaolinite is a high defect kaolinite and its crystallinity index of the studied samples calculated from the XRD pattern (Figure 1) is 0.28 which is comparatively low [15].

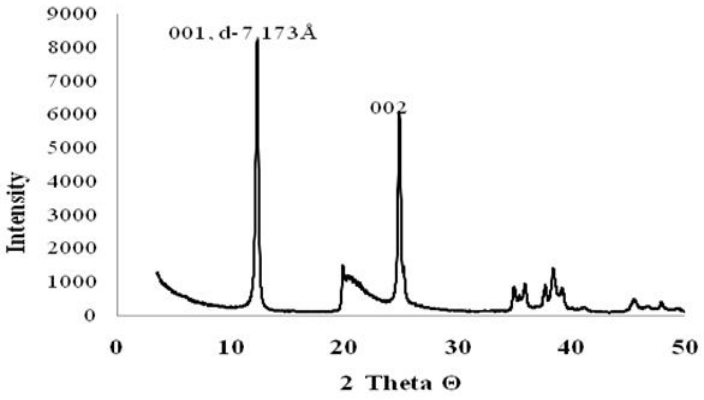

Figure 1: X-ray diffraction pattern from investigated sample GKa-2 (powder diffraction)

Electrokinetic potential (Zeta potential symbolised) was measured on the clay samples using Zeta size (Nano Series), manufactured by Malvern Ltd., UK. Samples of diluted suspension (~0.2 wt. %) prepared from the clay fraction and inserted to the disposable cell for measurement. The zeta potential of the studied kaolinite in DI water was -17 mV, in 0.01 M NaCl, was -10 mV, in pH ranging from –10 mV in low pH (pH 3) to -23 mV in high pH (pH 9) in water. XRD patterns were recorded with a PA N analytical X 'Pert Pro, multi-purpose diffractometer using Fe filtered Ca Ka radiation, auto divergence slit, 2° anti-scatter slit and fast X'Celerator Si strip detector.

The diffraction patterns were recorded in steps of 0.016° 2-theta with a 0.4 second counting time per step, and logged to data files for analysis. Electron microscope investigation was conducted using a JEOL-2100 Transmission Electron Microscope (TEM) with 200 kV accelerating potential. Scanning Electron Microscope

(SEM) JEOL 6040 was used to investigate samples coated in platinum film with accelerating voltage 15-20 kV. The field emission scanning electron microscope Philips XL30, FESEM with Oxford CT 1500HF Cryo stage The sample is fracture d under vacuum and a small amount of vitrified H2O sublimed off by raising the stage temperature to 90°C for ~30 s. Transmission X-ray Microscopy (TXM) proved to be an efficient instrument for three dimensional structural study of nano-materials owing to its large penetration depth and superior spatial resolution. TXM has been installed on the synchrotron of NSRRC in Taiwan. This TXM provides a two-dimensional imaging and three-dimensional tomography at energy between 8-11 ke V with a spatial resolution of 50-60 nm, and with the Zernike-phase contrast capability for imaging light material which lacks X-ray absorption contrast. TXM allows the study of any aqueous specimen because there is no need for a vacuum.

The photon energy of 8 ke V was used to image the clay suspension for the maximum X-ray absorption. The exposure time of a 2D image is from 15 seconds to 4 minutes. By acquiring a series of 2D images with the sample rotated stepwise, 3D tomography datasets are reconstructed based on 141 sequential image frames taken in the first order diffraction mode with azimuth angle rotating from -70º to + 70º for our lateral plate specimen. Images from all microscopy studies were statistically analysed using the STIMAN technique. The Statistical Image analysing system (STIMAN) has been adopted for the purpose of this study of clay suspensions. The STIMAN technique can extract integrated information on the sample microstructure, especially on total pore space and the spread of micro pore sizes. It contains a subroutine for estimating filtration properties from the void space parameters. Examples of the output parameters include: voids number analysed; porosity (%); total void/particle area (sq. μm); total void perimeter (μm); average diameter (μm); average perimeter (μm) and the form index (Kf) which is the platelet thickness. Form index is 1 for perfectly round isometric particles and nears 0 for string like, elongated particles.

In the present study, we use the STIMAN technique to obtain statistical information about porosity, particle average diameter and pore distribution accordingly to their total area from 2D micrographs and for the first time we adapt STIMAN technique to estimate in situ floccs relative density distribution and floccs dimension as an effect of suspension with different treatments. The 3D STIMAN technique was also used to estimate floccs size which is very difficult to determine without breaking the fragile aggregates (TXM investigations were undertaken in static mode without disturbing the sample). For this purpose two consequent TXM images with specific angle difference were investigated in the stereo image mode. TXM images as shown in Figure 1A, are space images, and carry information about the suspension layer which remains in focus in about 50 μm thick layer. Because all samples are uniform in mineral and chemical composition, the only differences obtained from images collected from different rotation angle, can be information about floccs packing density. As differences in density, in environment where only components which differ in density are water and the mineral skeleton, the variation of density can be understood as floccs sizes. In this way, information about space particle packing can be transposed from 3D space image to 2D height map (Figure 1B) where the lighter coloured spots represent higher density areas (larger aggregates) and darker spots represents low density area (smaller aggregates) in the flocc suspension. Such a map can display a graph which gives information about flocc dimensions.

This method is able to measure flocc dimensions in the range from 100 nm, which is near to the TXM resolution limit to few μm and complements the X-ray low angle scattering method which is suitable for measuring much smaller aggregate dimensions which is below the resolution of TXM method. Information about relative flocc dimensions can help in the comparison of different treatment results. The median height can give information about aggregate flocc dimensions and the maximum height value provides the flocc size range. The middle part of the height curve (after removing the lower and higher tails) represents the slope and carries information about uniformity of the flocc size distribution. When the slope is low, aggregate dimension is more uniform in comparison to higher slope values where aggregates show broader size distribution. The TXM images were collected from the KGa-2 sample in 10 wt. % aqueous suspension. The sample was dispersed in deionised water (DI), and limited treatment consists of changing the pH towards 2 and 9, undergoing sonication during 30 second with microwave treatment. Other treatments included the addition to the kaolinite suspension low and high anionic poly acryl amide flocculent and also 3wt. % of Smectite SWy-2 as described by Van Olphen and Fripiat, (1979) [4].

For better visibility of graphics, all information about samples was reduced to alphabetic letters which carry code information about sample treatment:(A)- dispersed in DI water, (B)- dispersed in DI water pH2, (C)- dispersed in DI water pH9, (D)- treated by microwave in DI water, (E)- treated by microwave in DI water pH2, (F)- treated by microwave in DI water pH9, (G)- treated by ultrasound in DI water, (H)- treated by ultrasound in DI water pH2, (I)- flocced by low anionic flocculent, (J)- flocced by high anionic flocculent, (K)- after addition of 3 wt.% of SW y montmorillonite in DI water, (L)- after addition of 3 wt.% of SW y monmorillonite in DI water treated by ultrasound.

Results and Discussion

The XRD pattern of the kaolinite sample is shown in Figure 1 and displays almost pure kaolinite with two distinctive 001 (hkl) peaks at 7.173 Å and at 002 (hkl) 3.577 Å with ramping or “tailed” pattern which follows 020 (hkl) peak at 4.46 Å of d space and 20o-23o (2Θ) which becomes increasingly blurred. Such a pattern when the first order spacing is slightly higher than d-space of 7.15 Å in highly crystalline kaolinite, suggesting some interlayer water between kaolinite units (Grim, 1968), and can be

regarded as the result of increasing stacking disorder [16]. Characteristic of poorly crystalline kaolinite Euhedral appearance of kaolinite crystals as mentioned by van Olphen and Fripiat (1979) [4] with the existence of an infrared band at 3669 cm-1 advocate that this kaolinite sample is not disordered and contains an admixture of highly ordered kaolinite. Results of electron microscope morphology studies and elemental composition are shown in Figure 3. Transmission Electron Microscopy (TEM) micrograph (Figure 2A) shows kaolinite euhedral crystals in the form of relatively small platelets displaying pseudo-hexagonal symmetry Most platelets are below one micron in size. Some of the platelets edges are eroded and poorly defined. Individual crystals can be up to 0.5 micron in diameter and smallest observed were only 50 nm in diameter. Most of the observed platelets were between 100-250 nm in diameter.

Most platelets are singular crystals but many form an assembly of larger aggregates and stacks. Stacks are primary crystals which are in the process of defoliation and can be seen occasionally. Such stacks observed in the SEM micrograph (Figure 2B) are up to 2 um in diameter and are 500 nm thick, which give the aspect ratio (ratio of diameter to thickness) of 2-4 which is much smaller than the typical kaolinite aspect ratio around 10. Most clay platelets are relatively small with average diameter calculated from TEM micrographs about 250 nm. Other minerals spotted in the TEM micrographs are small anatase crystals about 100 nm in diameter.

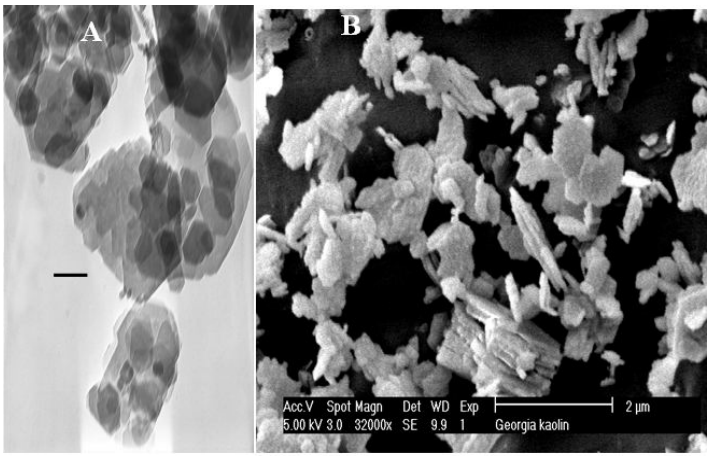

Figure 2: Electron microscope micrographs displaying morphology and aggregate geometry of studied GKa-2 kaolin sample. (A)- TEM micrograph show pseudo-hexagonal euhedral kaolinite crystals of lateral dimension from 50 to 500 nm (scale 200 nm). (B)- Cryo-SEM micrograph show aggregate geometry where individual platelets and small stacks connecting each other in FF and FE contacts and forming broad range interconnected aggregates.

The Cryo-SEM micrograph in Figure 2B displays kaolinite particles in vitrified DI water suspension partly protruding from the sublimated ice layer. Most kaolinite platelet-like crystals and stacks, assemble in small aggregates in which platelets are mostly in Face to Face (FF) and Face to Edge (FE) contacts. Most of aggregates were about 1 µm in diameters and display significant variation in these dimensions. The TXM micrographs shown in Figure 3 display 3D microstructure of 12 samples representing different treatments of kaolinite samples in 10 wt.% aqueous suspension. Each of the TXM micrographs has a 2D frame dimension of 16x16 µm. All displayed micrographs look similar in the term of texture morphology. They show long chains of interconnected kaolinite platelets which forms spanned network. Porosity calculated from TXM space micrographs ranging from 10 to 25 % and voids average diameter vary between 220 to 380 nm, positive correlation between these values was observed (Figure 4) which increases in following row: (C)- dispersed in DI water pH9>(D)- Micro waved>(B)- dispersed in DI water pH2>(K)- with addition of Smectite SW 3%>(I)-low anionic poly acryl amide flocculent>(E)- Micro waved pH2> (F)- Micro waved pH9>(J)- high anionic poly acryl amide flocculent>(L)- with addition of Smectite SW 3% sonicated > (A)- dispersed in DI water>(G)- sonicated in DI water> (H)- Sonicated pH2.

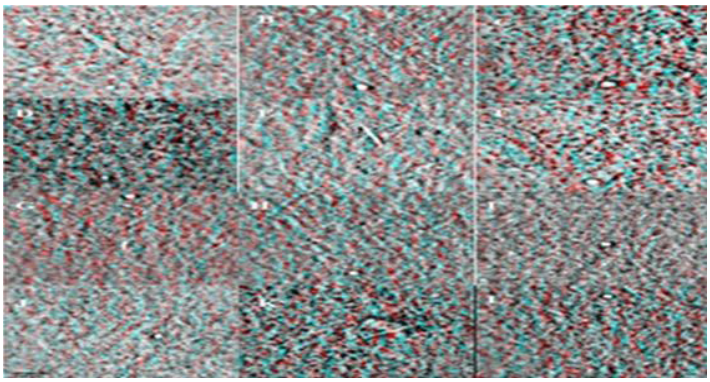

Figure 3 : TXM anaglyphic micrographs of kaolinite flocculated microstructure in; (A)- dispersed in DI water, (B)- dispersed in DI water pH2, (C)- dispersed in DI water pH9, (D)- treated by microwave in DI water, (E)- treated by microwave in DI water pH2, (F)- treated by microwave in DI water pH9, (G)- treated by ultrasound in DI water, (H)- treated by ultrasound in DI water pH2, (I)- flocced by low anionic flocculent, (J)- flocced by high anionic flocculent, (K)- after addition of 3 wt.% of SWy montmorillonite in DI water, (L)- after addition of 3 wt.% of SWy montmorillonite in DI water treated by ultrasound

The Transmission X-ray Microscope space micrographs as shown in (Figure3) were typical for all studied samples using this method. In these (positive) micrographs, white kaolinite mineral particles can be observed. These particles are plates as observed in the electron microscope micrographs (Figure 2) and connected to each other mostly by edges forming longer chains and spanned all suspension within the3D frame(16 x 16 x 50 µm).Between platy particles empty space, voids or pores can be observed. Many of these inter particle voids have geometrically angular shape limited by platy mineral skeletons. These angular voids were mostly filled with water and can be seen as grey in colour. For the X-ray absorption, there is little difference between clay silicates and water, so

phase contrast mode employed in the TXM significantly increase mineral/water weak phase contrast. Thanks to combination of absorption and phase differential modes, the gray colour differences between silicate particles and water filled pores can be recognised. However, contrast is weak and micrographs obtained may always be electronically enhanced for better visibility prior to statistical analyses. This may be a source of an uncertain error.

In the TXM micrographs, a certain amount of clearly visible black areas was observed. They were treated as voids, but most of these black areas have distinguishable spherical shape or chain-like of spherical beads. As the spherical voids are unlikely to occur within assembly of platy particles it is most likely that they are the air bubbles trapped within spanned platelet space network. Deeper black colour of these bubbles may be due to lack of X-rays absorbance travelling through an air. All observed micro-bubbles, similar to larger mineral skeleton particles looks to be arrested within the network and have not been able to move (float in case of bubbles or sediment in case of larger mineral particles) because of the hindering viscous behaviour of clay gelled particle network. Micro-bubbles associated within clay suspensions and aggregates have already been reported Żbik et al. (2010) [17].where air micro-bubbles and air blankets frequently covering kaolinite/water interface. Keeping all this uncertainty in mind, our porosity results reported in this contribution combine voids filled with air and water. Also, it has to be understood that the TXM space picture contain information from about 50 µm of suspension structural elements which stay in focus through all this distance which is much larger than the 2D frame dimension (16 x 16 µm). So, many particles and pores obscure each other giving much reduced porosity values. These data, however, can be used as comparative information between samples and their treatment results. Kaolinite suspension in water (Figure 4A) display a network of flocced aggregates connected in all possible contacts.

Floccs display a random mixture of dimensions and are interconnected by short chained platelet aggregates. Highly circular voids suggest pockets of air trapped within clay network. Porosity value is rather high 21.6 % and average void diameter is 350 nm. From the pore size distribution (Figure 5A) it is understood that poorly defined multimodal curve shows very broad pore population in a large range between 400 and 1400 nm. From 3D stereoscopic spectroscopy of TXM images (heights graph Figure 7A) the median flocced aggregate size was estimated on 970 nm and broad range of flocced aggregates range from the resolution limit about 100 nm to 2300 nm with the steep slope testify of highly diverse flocc distribution range.

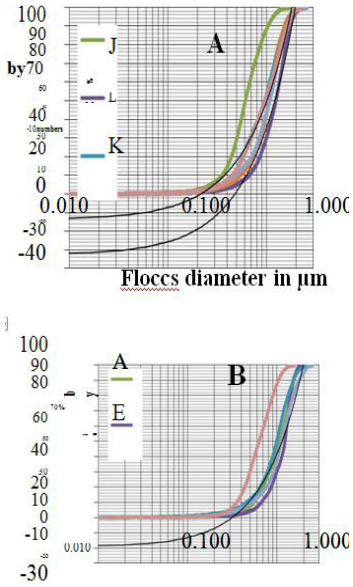

Figure 4: The floccs size distribution from the heights maps studied from 3D images of studied samples

Treatment by pH changes

Treatment based on lowering the suspension pH, decrease platelets mostly in EF contacts assembling smaller floccs. Porosity values drop to 11.5 % and the average pore diameter to 240 nm. In the pore size distribution curve, major peaks narrow and shift towards lower size values (450 nm). In terms of microstructure (Figure 3B), aggregates form interconnected long chains of platelets in stair step FF and FE orientation building cellular structure with slightly elongated voids. Treatment based on increasing the suspension pH, increased interconnected chain length with increasing larger inter-aggregate pores at the expense of smaller intra-aggregate voids. Total porosity slightly was lowered in comparison with the measured at pH 2, to about 10% but the average pore diameter stays around 250 nm.

The pore size distribution show clear multimodality and division between intra aggregate pores with diameters around 450 nm and much larger voids, up to one micrometer, which occupied the space between floccs. Microstructure as observed in Figure 3C show long chained aggregates mostly EE connected and zigzagging around elongated voids which most probably were filled by a mixture of air and water. In flocc size distribution diagram (Figure 4A) the natural kaolinite sample dispersed in DI water displays slightly lower value of the median size floccs (970 nm) in compari-

son with suspensions treated at different pHs. This sample (A) also was characterized by a larger slope value in comparison with all the studied samples. Such micro structural parameters suggest that highly porous non-treated kaolinite suspensions have the broadest aggregate size range, which were in the majority of slightly lower dimension than those in pH treated samples.

Treatments of this suspension by changing its pH resulted in improved uniformity of aggregates (low pH) size distribution with lower porosity and pore average diameter. Larger inter-aggregate pore population increased with increase in flocc density in the higher pH samples. Both natural non-treated kaolinite dispersion and high pH treated samples display multimodality as observed in Figure 5A with broader shift in voids sizes either into lower and higher diameter values. Aggregates in pH treated kaolinite samples become slightly more compact (increase median heights) and more uniform in their dimension distribution range (lower slope) in comparison with non-treated kaolinite sample with aggregate size with a wider range. As all structural elements like voids and mineral phase relate to each other, their sizes may also be related. In the non treated suspension, pore and aggregate sizes display broad dimension range, however after lowering H smaller pores and smaller aggregates dominate flocced suspension and larger pores with larger flocced aggregates were formed at high pH Similar findings have been found previously when studied pH treated kaolinite suspension in Cryo-SEM method [14].where more compact aggregates and larger inter-aggregate voids were observed in kaolinite flocculation at pH 8.

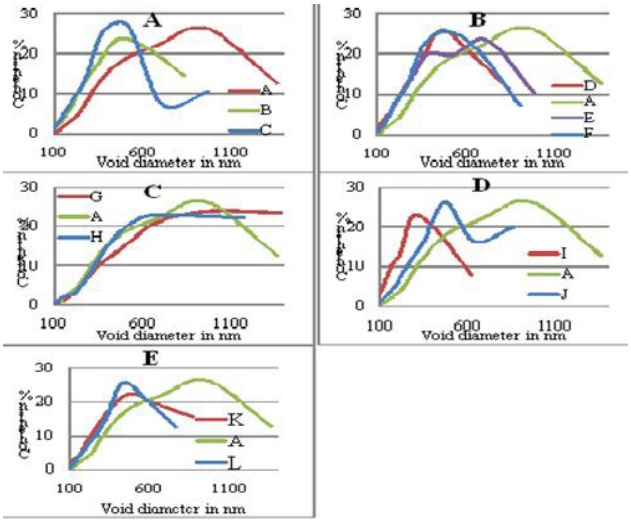

Figure 5: Total void content distribution according their diameters; calculated from TXM images in Figure3 (A)- in DI water with pH changes, (B)- microwave treated, (C)- ultrasonic treated, (D)- flocculent treated, (E)- with smectite addition.

Effect of Microwave action

Kaolinite suspension treated with microwave action, display mostly porous small and fluffy EE connected floccs interconnected in spacious uniformly sized network. Total porosity11.3 % and the average void diameter 260 nm were lower in comparison to the same parameters of non-treated kaolinite sample. The pore size distribution (Figure 6B) in microwave treated kaolinite suspension displays much narrower and higher peaks with the maximum shifted from 960 nm measured in non-treated sample in DI water to around 460 nm in kaolinite after microwave treatment. Such a porosity reduction and peak narrowing is due to air micro bubbles significant reduction or removal. From height distribution reassembling suspension floccs sizes (Figure 4) significant drop of flocc size either in median floccs diameter (630 nm) as well as in total range of floccs size distribution testify of aggregate dispersion in comparison with measurements done in DI water.

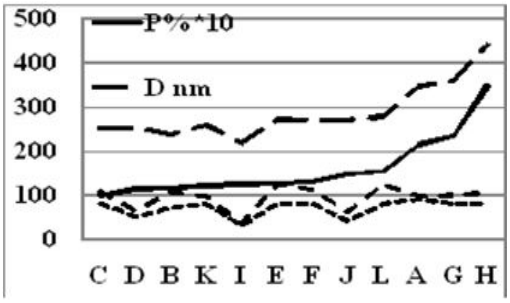

Figure 6: Values of: porosity (P- in %+10), average voids diameter (D-nm), median heights from 3D maps (in nm) and slope angle parameter

The pH changes in microwave treated suspension microstructure slightly increases the average pore size to P- 12.5 %, 270 nm at low pH and 13 %, 270 nm at high PH. Microwave treated sample at low pH show (Figure 5B), broad pore size distribution with two distinctive pore diameter maxima at 400 nm and 700 nm. In high distribution curve (Figure 4B) the median value of floccs sizes increases to a high value (1230 nm) which proves twice larger particles agglomeration in comparison to non-treated microwave samples. The low slope value may be interpreted as narrow range of floccs sizes distribution. In microstructure observed in Figure 3E, cellular network is apparent and consists with short thick chain oh EF connected platelets and interconnected forming slightly elongated voids.

Microwave treated sample at high pH show long ribbon like interconnected compact FF and FE connected kaolinite platelets. Chain aggregate observed in Figure 3F are much thinner and voids surrounded by these chained aggregates look longer in comparison with those observed at low PH. Total porosity 13% displayed in Figure 5B, show broader major peak appear narrow in comparison with other microwave treated samples and displays multimodality in void diameter distribution which may be an effect of larger intra-aggregate voids appearing between long and compact ribbons-like flocced aggregates. In the high distribution curve (Figure 4) the median value of floccs sizes (1120 nm) was larger than in the sample microwave treated in DI water and slightly smaller than those measured at lower pH This suggests particle agglomeration.

Examined curves of microwave treated suspension at higher pH, displays slightly higher slope value in comparison with microwave treated sample in DI water at low pH, which is interpreted as broader ranges of floccs sizes.

Effect of Ultrasonic treatment

The ultrasonic treatment in micrograph Figure 3G displays highly interconnected cellular microstructure of short chained platelets mostly connected in FF contacts. Well observed spherical voids within voids may suggest air bubbles trapped within the network. Porosity has increased values to 23.5% and an average pore size of 360 nm was comparable with values measured in the DI water of natural pH Porosity value increases to 35% in suspension sonicated at lower pH and the average pore size has risen to 440 nm which suggests aggregate compacting (for technical reasons we didn't get reliable results from high pH suspensions). In general, kaolinite suspension treated by ultrasonic action, do not display dispersion of aggregates as seen from pore distribution diagram in Figure 5C where peaks maximum do not exists and curves were open and tailings towards larger void diameters. This may occur because mineral interface was cleaned by gaseous blankets (below TXM detection limit) and all air component form micro-bubbles (well visible in TXM images) increasing measured porosity value. Similar process of cleaning clay particles from gaseous component and remove from low solid packed suspension was described in Żbik et al (2010) [17]. In case of dense clay suspensions, this gaseous component whipped out from mineral interface formed micro-bubbles which were trapped within the network of gelled suspensions without the possibility of removal from the gelled system. Microstructure in natural and low pH looks similar with slight drop of average pore size in low pH sample. However, as seen in Figure 3H flocced aggregates were longer and elongated inter-aggregate voids were observed.

The median value from the flocc size distribution in non-treated and sonicated samples look very similar (Figure 4B) with a very small increase in aggregate size, after sonication as median heights value rise from 970 nm in non treated water suspension to 990 nm in the sonicated suspension. The median height value in sonicated kaolinite suspension at low pH shows small increase of flocc size to 1040 nm suggesting aggregation. Sonication, in view of aggregate size distribution, is not so effective in aggregate dispersion, when compared with microwave treatment which has much stronger impact on aggregate size decrease.

Effect of Flocculent addition

The flocculent addition show largest impact on kaolinite suspension producing fine cellular microstructure (Figure 3I-J).Sample porosity, after low anionic flocculent addition ,displays low values P- 12.4 % and average pore diameter 220 nm and P- 14.9 % and average pore size 270 nmin high anionic polymer treatment.

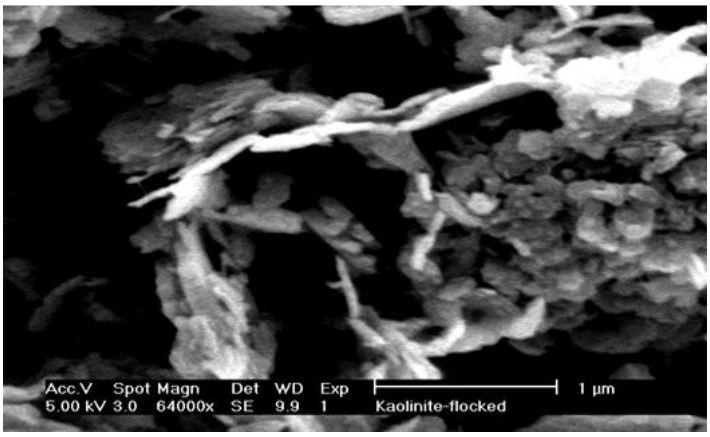

Figure 7: Single platelet E-E contacted chain associations in kaolin based suspension after flocculent addition preserves previously existing high porosity structure

Microstructure of this sample as observed in Figure 3I (low negatively charged polymer) looks much different to most samples and display similarities to sample treated by microwave action. Characteristic by highly cellular space network of fluffy short chained EE connected aggregates of very uniform size distribution within the studied area. In highly negatively charged polymer observed in Figure 3J, the sample shows smaller uniformly shaped cellular network. The pore size distribution in polymeric flocculent treated kaolinite dispersion (Figure 5D) displays narrowing and a shift pore size distribution peaks maxima towards smaller voids diameter at 290 nm in low anionic polymer and 470 nm in high anionic polymer with curve tailing towards higher pores diameters probably responsible for inter floccules pore spaces. The high anionic polymer displays more complex influence on suspension microstructure by broadening peaks and much clear display peak multimodal character. Because the lower limit in voids, measurement was about 100 nm, these smaller voids distribution component may be underestimated. In the height distribution curves (Figure 4A) kaolinite suspension treated by low anionic polymer display lower median flocc sizes (350 nm) and the lowest floccs maximum size range (1130 nm). Kaolinite suspensions treated by high anionic polymer display almost twice the larger median flocc size value (610 nm) and larger maximum aggregate size range dimension (1740 nm).

In both samples the slope looks similar and testifies for high uniformity in aggregate size distribution range. Most structural elements like voids and particle or aggregates having close similar sizes, the voids size distribution major peak at 290 nm in low anionic polymer treatment may be coincident with median aggregate size 347 nm and major peak in high anionic polymer treatment at 470 nm may coincident with median aggregate size 610 nm taken from median height value distribution. It may be against logical thinking to conclude that polymeric flocculants diminish-

ing the aggregate size and so the flocc density instead of increasing them. Results without any doubt, testify that polymeric flocculent used in the present study did not density or enlarge the flocced aggregates. In contrary polymer fixed primary aggregate size and prevent further particle agglomeration freezing the pre-existing structure. Similar conclusions were drown from Cryo-SEM investigation of the kaolinite flocculation structure in previous work Żbik et al (2009),[18] so this observation got confirmation from another independent TXM image analysing method. In Cryo-SEM micrograph (Figure 7) it is recognisable that kaolinite individual platelets and small aggregates were connected in EE contacts giving a very porous microstructure. Because particles were bonding to each other by steric action of the polymer, structure is set and particles cannot relocate freely to build more compact FF connected aggregates. Any attempts to grow larger aggregates within suspension, have to be done during primary dewatering and before flocculent addition.

Effect of Smectite Addition

A previous study suggests that a small addition of s mectite in the kaolinite dispersion can help in aggregation and increases the settling rate which may be helpful in clay particle agglomeration [15].The grew test impact on kaolinite flocculation was observed in 3 wt. % of s mectite addition to the 10 wt. % dense clay suspension. To check these findings, new samples were studied and investigated using TXM and 3D STIMAN technique.

Kaolinite suspension microstructure has been described in detail Żbik et al. (2010) [15] in kaolinite–s mectite suspensions, s mectite form highly oriented basic framework into which kaolinite platelets were bound in face to face preferential contacts strengthening structure and allowing them to show plastic behaviour which causes structure orientation. In Figure 3K, highly porous channel-like oriented network of pores, were surrounded by chained and randomly rather than oriented particles. The porosity value shows a decrease from ~22% in non treated suspension in DI water to 12% after addition of small amounts (3 wt.%) of s mectite and the average void diameter also decreased from 350 nm in non treated samples to 260 nm after s mectite addition. Pore size distribution as observed in Figure 6E, show mono modal curve displaying smaller maximum at 480 nm with extended tailing towards larger void diameters. After ultrasonic treatment of this kaolinite with s mectite (K-S) addition suspension, porosity further decreased to 15.4 % with slight increase of average void diameter 280 nm. In pore size distribution the ultrasonic treatment of K-S suspension narrowed and shifts the main peaks left, towards smaller diameters (with maximum at 440 nm).

In the structural terms network shown in Figure 3L looks having much longer chained aggregates connected mostly in EE orientation Channel-like inter aggregate voids also seem to be longer than before ultrasonic treatment. From floccs distribution curves (Figure 4A) can be deducted that curve of kaolinite dispersed in DI water is somehow similar to kaolinite suspension sample with 3 wt. % of s mectite addition. Also median heights parameter is almost identical at 960 in non treated DI water to 970 nm in K_S suspensions. The only difference is in curve slope which is lower after s mectite addition proving a more uniform aggregate size distribution. Ultrasonic treated suspension of kaolinite with s mectite addition, show particle agglomeration through rising median value to larger value from all samples studied, at 1245 nm. This is understood as a significant aggregation agent. Interestingly, maximum aggregate dimensions remain exactly the same in both Smectite treated samples and only slightly smaller in comparison with non-treated kaolinite suspension.

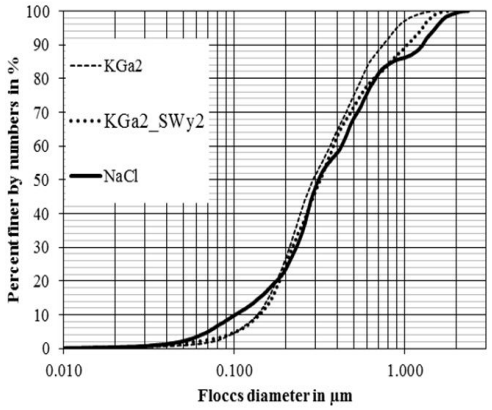

Figure 8: The flocc size distribution from 3D images of studied samples shows larger percentage of smaller particles in sodium Smectite up to about 175 nm in diameter in comparison with these in kaolinite suspension.

The flocc size distribution (Figure 8) obtained from 3D images of studied kaolinite and kaolinite treated by small Smectite addition samples shows a larger amount of smaller particles in sodium Smectite in diameter range up to about 175 nm in comparison with particles within this range in kaolinite suspension. Flocc diameter in the higher range of particle diameters is a few percent larger in kaolinite gelled suspension in comparison with Smectite and kaolinite suspension treated with Smectite addition. The kaolinite suspension treated with Smectite addition, follows a trend similar to the Smectite flocculation pattern. The only difference between these curves was in a smaller percentage of particles in the range up to 175 nm inthe kaolinite suspension treated with Smectite addition and broader range in floccs dimension within sodium Smectite gelled suspension.

Conclusions

Investigation of the dense kaolinite aqueous suspensions were studied with the use of synchrotron powered Transmission X-ray Microscope giving important new information on the micro structural behaviour of clay aqueous systems and help to find how different treatments may influence the system properties. Kaolinite platelet-like particles and aggregates as displayed in 3D anaglyph

micrographs, show microstructure in which mineral particles were connected to each other with collaborate EE and FE contacts configuration, forming interconnected chains, which span three-dimensional network through all observed sample volume. In such a network, all mineral particles, even much larger than clays, were immobilised by hindering action of neighbour network particles, scaffolding all gelled systems. Inter-particle voids observations and measurements in TXM space images were found to be filled with water. Some assembly of complex liquid/gaseous environment in form of gaseous envelopes on mineral interfaces and in the form of micro-bubbles were observed. These micro-bubbles, similarly to larger mineral particle, looks to be arrested within the network and not been able to move (by floating them up towards the surface) because of hindering viscous behaviour of clay gelled system. The air bubbles arrested within this network plays the role of additional buoyancy. Such air bubbles in addition to hindering support of mineral skeleton within clay suspension, prevents particles from settling by building addition buoyancy force which works against gravitation. Existence of such air filled voids needed to be independently confirmed using other methods. To confirm our findings the Cryo-FIB/SEM examination of clay dense suspension is now planned.

Different ways of kaolinite suspension treatment were found to impact on gelled clay system microstructure; however, none of the used methods was able to destroy the spanned clay network, which seemed to be the major factor of poor particle settling and sludge dewatering. Large porosity values were measured in kaolinite suspension dispersed in DI water (A) and gaseous component plays important role in this sample. The void dimension also shows comparatively large values with broad range of pores diameter. The highest slope value of flocc distribution in this sample and relatively large median flocc dimensions may testify the highly uneven structural elements distribution in this suspension. Ultrasonic action increases the porosity values which most probably was affected by removing air envelope from the mineral interface and produce more micro-bubbles, which were trapped within gelled network. This treatment increases the porosity value as well as the average pore size by disintegrating the major aggregates. So, ultrasonic action which was found to help in cleaning mineral/water interfaces in clay low density clay suspensions is not suitable for the removal of micro-bubbles from gelled dense clay systems. The ultrasonic treatment has little effect on the smaller flocc size, but low slope value can testify that flocced aggregates were more uniformly distributed in the ultrasonic treated suspension.

The microwave treatment did have to some extend impact on kaolinite suspensions by lowering floccs/aggregate size, and void average diameter. The decrease of the flocc median size and slope angle may testify the aggregate uniform size distribution. Flocc dimension were larger in low pH microwave treated suspensions. This may suggests that microwave treatment at higher pH may be the most effective method to disperse aggregates with in high density kaolinite suspensions. Perhaps this treatment with simultaneous ultrasonic action can be seen as worth to follow in the design of particle dispersing technology. Flocculent treatment of dense kaolinite suspensions is more complex and not yet understood. The low negatively charged flocculent addition influences the most important changes in suspension microstructure. It was noticed the high porosity drop with coincidence with largest drop of voids average size as well as lowering value of the median floccs sizes and the lowest value of the slope angle. These treatments may produce small and uniformly distributed floccs of very narrow sizes range distribution. The short chain EE connected platelets, seen in SEM micrographs, were coiled by polymer and prevent from any further aggregation by steric action of a polymer itself. The highly negative flocculent did not have such dramatic impact on kaolinite suspension showing moderate influence on porosity and pore size drop. The only similarity between both used flocculants was the lowest slope angle value, which tells of high uniformity of the narrow floccs size range. This may happening because aggregates were immobilised by polymer which prevents particles against further aggregation.

Small amount of Smectite addition into kaolinite dense suspension lowers the porosity and pore average diameter without influence of the flocc size median value. It is possible that Smectite nano-particles can contribute to kaolinite aggregate building phenomenon, as in kaolinite-Smectite mixture nano-in size particles show deficiency in comparison with sodium Smectite sample. Lowering the slope value may testify to a more uniform floccs distribution. The kaolinite with Smectite addition suspension treated by ultrasonic action causes flocc aggregation No change in slope value suggests that densification of floccs during sonication was uniform for all range of aggregate sizes. All treatment results obtained from kaolinite dense suspension can be used for comparison. These findings significantly contribute to establishing technology of an efficient method for air removal from clay spanned network and the network rebuild to form compact FF contacted aggregates and contribute to the settling rate improvements and increased efficiency of sludge dewatering which is important issue for mining industry in tailing management.

All results advocate, the structure building phenomenon within entire suspension may be blame for poor settling and dewatering. All these may be result of high water dielectric constant which polarising clay particles and generating electrostatic charge. This charge leads to structure building phenomenon within the aqueous suspensions. It becomes clear that further technologies have to eliminate using water in mineral processing and develop new approach involving close loop processing environment in low dielectric constant liquids.

References

1. Grim RE (1968) In: Clay Mineralogy. McGraw-Hill, New York, 596.
2. Braggs B, Fornasiero D, Ralston J, Smart ST C (1994) The effect of surface modification by an organosilane on the electrochemical properties of kaolinite. Clays and Clay Minerals 42: 123-136.
3. Jepson WB (1984) Kaolins: their properties and uses. Philosophical Transactions of the Royal Society of London A31: 411-432.
4. VanOlphen H, Fripiat JJ (1979) Data handbook for clay minerals and other non-metallic materials, Pergamon Press 346.
5. Kotlyar LS, Sparks BD Le Page JR (1998) Effect of particle size on the flocculation behavior of ultrafine clays in salt solutions. Clay Minerals 33:103-107.
6. NROBrien (1970) Journal of Electron Microscopy 19: 277.
7. Zbik MS, Smart R St C, Morris GM (2008) Kaolinite flocculation structure. Journal of Colloid and Interface Science 328: 73-80.
8. Zbik MS, Frost RL (2009) Micro-structure differences in kaolinite suspensions. Journal of Colloid and Interface Science 339: 110-116.
9. Kotlyar LS, Sparks BD, Schutte R (1996) Effect of salt on the flocculation behavior of nano particles in oil sand fine tailings. Clay and Clay Minerals 44:121-131.
10. Kotlyar LS, Sparks BD, Le Page Y, Woods JR (1998) Effect of particle size on the flocculation behaviour of ultra-fine clays in salt solutions. Clay Minerals 33: 103-107.
11. Yin GC, Tang MT, Song YF, Chen FR, Liang KS, et al. 2006) Energy-tuneable transmission X-ray microscope for differential contrast imaging with near 60 nm resolution tomography. Applied Physics Letters 88:241115- 1-241115-3.
12. Attwood D (2006) Nanotomography comes of age. Nature 442: 642-643.
13. Niemeyer J, Thieme J, Guttmann P, Wilhein T, Rudolph DG (1994) Direct imaging of aggregates in aqueous clay-suspensions by X-ray microscopy. Progress in Colloid and Polymer Science 95: 139 - 142.
14. Zbik MS, Frost RL, Song YF (2008) Advantages and limitations of the synchrotron based transmission X-ray microscopy in the study of the clay aggregate structure in aqueous suspensions. Journal of Colloid and Interface Science 319:169-174.
15. Hinckley DN (1963) Variability in “Crystallinity” values among the kaolin deposits of the Coastal Plain of Georgia and South Carolina. Eleventh National Conference on Clay and Clay Minerals 229-235.
16. Brindley GW, Brown G (1980) Crystal Structures of Clay Minerals and their X-ray Identification Mineral Society London 495.
17. Zbik MS, Song YF, Frost RL (2010) Kaolinite flocculation induced by Smectite addition – A transmission X-ray microscopic study. Journal of Colloid and Interface Science 349: 86-92.
18. Zbik MS, J Du, Pushkarova RA, Smart RStC (2009) Observation of gaseous films at solid–liquid interfaces: Removal by ultrasonic action. Journal of Colloid and Interface Science 336: 616-623.